Effects of myosin heavy chain (MHC) plasticity induced by HMGCoA-reductase inhibition on skeletal muscle functions

Laura Trapani,*[,1] Luca Melli,[†,1] Marco Segatto,*[,1] Viviana Trezza,* Patrizia Campolongo,[‡] Adam Jozwiak,[§] Ewa Swiezewska,[§] Leopoldo Paolo Pucillo,[#] Sandra Moreno,* Francesca Fanelli,* Marco Linari,[†] and Valentina Pallottini*[,2]

*Department of Biology, University of Roma Tre, Rome, Italy; [†]Department of Evolutionary Biology, University of Florence, Florence, Italy; [‡]Department of Physiology and Pharmacology, University of Rome La Sapienza, Rome, Italy; [§]Institute of Biochemistry and Biophysics, Polish Academy of Sciences, Warsaw, Poland; and [#]National Institute for Infectious Diseases, Rome, Italy

ABSTRACT **The rate-limiting step of cholesterol biosynthetic pathway is catalyzed by 3-hydroxy-3-methylglutaryl coenzyme reductase (HGMR), whose inhibitors, the statins, widely used in clinical practice to treat hypercholesterolemia, often cause myopathy, and rarely rhabdomyolysis. All studies to date are limited to the definition of statin-induced myotoxicity omitting to investigate whether and how HMGR inhibition influences muscle functions. To this end, 3-mo-old male rats (*Rattus norvegicus*) were treated for 3 wk with a daily intraperitoneal injection of simvastatin (1.5 mg/kg/d), and biochemical, morphological, mechanical, and functional analysis were performed on extensor digitorum longus (EDL) muscle. Our results show that EDL muscles from simvastatin-treated rats exhibited reduced HMGR activity; a 15% shift from the fastest myosin heavy-chain (MHC) isoform IIb to the slower IIa/x; and reduced power output and unloaded shortening velocity, by 41 and 23%, respectively, without any change in isometric force and endurance. Moreover, simvastatin-treated rats showed a decrease of maximum speed reached and the latency to fall off the rotaroad (~−30%). These results indicate that the molecular mechanism of the impaired muscle function following statin treatment could be related to the plasticity of fast MHC isoform expression.—Trapani, L., Melli, L., Segatto, M., Trezza, V., Campolongo, P., Jozwiak, A., Swiezewska, E., Pucillo, L.P., Moreno, S., Fanelli, F., Linari, M., Pallottini, V. Effects of myosin heavy chain (MHC) plasticity induced by HMGCoA-reductase inhibition on skeletal muscle functions. *FASEB J.* 25, 4037–4047 (2011). www.fasebj.org**

Key Words: cholesterol · statins

THE MAIN PRODUCTS OF THE mevalonate (MVA) pathway—cholesterol, ubiquinone (CoQ), prenyl diphosphate, and dolichol—are essential compounds for survival, proliferation, and differentiation of all mammal tissues (1, 2). In skeletal muscle, cholesterol is essential for the propagation of action potentials along the cell (3). CoQ participates in electron transport during oxidative phosphorylation in mammalian mitochondria, ensuring the production of ATP needed for muscle contraction (4). Oligoprenyl groups are necessary for post-translational modification of proteins crucial for cell proliferation and differentiation; among others, the small Rho GTPases, able to activate Rho-associated serin/threonine kinase (Rho-kinase) (5). Lastly, dolichol is needed for *N*-linked glycoprotein biosynthesis (6).

The rate-limiting step of the MVA pathway, the 4-electron reduction of 3-hydroxy-3-methylglutaryl coenzyme A (HMG CoA) to MVA, is catalyzed by HMG-CoA reductase (HMGR). Thus, as the central regulator of cholesterol homeostasis, HMGR became the target for drugs that control plasma cholesterol levels. The enzyme is highly regulated; short-term regulation is achieved by phosphorylation/dephosphorylation reactions exerted by AMP-activated kinase (AMPK) and protein phosphatase 2A (PP2A), respectively. Long-term regulation concerns the modulation of HMGR protein levels by several factors, among others sterol regulatory element binding protein (SREBP) and insulin-induced genes (Insigs), which can affect enzyme transcription and degradation as a function of an intracellular sterol amount and of cholesterol uptake by low-density lipoprotein receptor (LDLr) (7).

Statins, strong HMGR competitive inhibitors widely used to treat hypercholesterolemia, besides the beneficial effects on plasma lipid profile, can cause myopathy characterized by weakness, pain, elevated serum creatine phosphokinase (CK) (2), and to a lesser extent (0.05%), rhabdomyolysis, a life-threatening condition (8). Moreover, previous data demonstrate that HMGR

[1] These authors contributed equally to this work.

[2] Correspondence: Department of Biology, University of Roma Tre, Viale Marconi 446, 00146, Rome, Italy. E-mail: vpallott@uniroma3.it

doi: 10.1096/fj.11-184218

is crucial for myoblast differentiation to occur (9); indeed, HMGR inhibition or down-regulation lead to both the reduction of muscle differentiation markers [myogenin and fetal myosin heavy chain (f-MHC)] and of myoblast fusion into multinucleated syncitia (9).

Although these combined findings bring out the importance of HMGR activity in skeletal muscle physiology, all the studies so far are limited to the definition of statin-induced myotoxicity, omitting to investigate whether and how the inhibition of HMGR activity influences muscle functions. Moreover, epidemiological studies show that some patients treated with statins complain of muscle pain without any increase in plasma content of muscle damage markers, such as serum CK (4), which suggests that HMGR inhibition could impair muscle function without exerting any muscle toxicity.

Here we studied *in vivo* the role of HMGR inhibition by simvastatin on skeletal muscle physiology through biochemical, morphological, mechanical, and functional approaches.

MATERIALS AND METHODS

Reagents

All chemicals were obtained from commercial sources and of the highest quality available. Sources not specified were obtained from Sigma-Aldrich (Milan, Italy).

Animals

Wistar *Rattus norvegicus*, 3-mo-old male (Harlan Nossan, S. Pietro al Natisone, Italy), were housed under controlled temperature (20±1°C), humidity (55±10%), and illumination (lights on for 12 h daily, from 7 AM to 7 PM). Food and water were provided *ad libitum*. The experiments were performed according to the ethical guidelines for the conduct of animal research (Ministero della Salute, Official Italian Regulation No. 116/92, Communication to Ministero della Salute no. 391/121). Rats were divided into 2 groups of 28 animals each. The first group was treated daily with intraperitoneal injection of 1.5 mg/kg simvastatin in vehicle [dimethyl sulfoxide (DMSO), 1 ml/kg] for 3 wk, a dose comparable to the highest one used in therapies against human hypercholesterolemia. Control animals received daily an equal volume of vehicle. At the end of the treatment, rats were anesthetized with ether in a fume cupboard, and plasma was obtained from blood collected into EDTA (1 mg/ml blood). Extensor digitorum longus (EDL) and gastrocnemius muscles of 7 animals/group were dissected and immediately frozen in liquid nitrogen for subsequent biochemical assays. Eight animals from each group were used for mechanical analyses; in particular, after dissection, EDL muscles were mounted in an experimental trough to analyze the contractile properties. For immunolocalization studies, EDL muscles from both sides of 3 animals/group were isolated and fixed by immersion in phosphate-buffered saline (PBS; pH 7.4) containing 4% freshly depolymerized paraformaldehyde, overnight at 4°C. For rotarod motor coordination test and open-field locomotor activity, 10 animals/group were used.

Biochemical analysis

Plasma cholesterol analysis

Plasma cholesterol content of rats was assessed through the colorimetric CHOD-POD kit (Assel, Rome, Italy) according to manufacturer's instructions. Briefly, by the catalysis of cholesterol esterase and cholesterol oxidase, cholesterol ester was catalyzed to yield H_2O_2, which oxidates 4-aminoantipyrine with phenol to form a colored dye of quinoneimine. The absorbancy increase is directly proportional to the concentration of cholesterol.

Tryglyceride and creatin kinase assays

Plasma triglyceride levels and creatin kinase activity were measured by standardized commercial methods on a fully automated system (Modular; Roche, Basel, Switzerland). Triglycerides are hydrolyzed to glycerol by lipoprotein lipase and oxidized to dihydroxyacetone phosphate and hydrogen peroxide, which reacts with Trinder reagent to form a red dye. The color intensity is directly proportional to triglyceride concentration. This method is linear between 4 and 1000 mg/dl. Activity of creatin kinase measurement is in accordance with the method recommended by the International Federation of Clinical Chemistry at 37°C.

HMGR activity

The assay was carried out with the radioisotopic method, following the production of [^{14}C]-MVA from 3-[^{14}C]- hydroxymethylglutaryl coenzyme A (3-[^{14}C]-HMGCoA; specific activity 57.0 mCi/mmol; GE Healthcare, Little Chalfont, UK). Microsomes were prepared as described previously (10) from gastrocnemius. Microsomes were incubated in presence of cofactors (20 mM glucose-6 phosphate, 20 mM $NADP^+$ sodium salt, 1 IU glucose-6 phosphate dehydrogenase, and 5 mM dithiothreitol). The assay, in a final volume of 200 μl, was started by the addition of 10 μl (0.088 μCi/11.7 nmol) of 3-[^{14}C]-HMG CoA. The [^{14}C]-MVA produced was isolated by chromatography on AG1-X8 ion-exchange resin (Bio-Rad Laboratories, Milan, Italy), and the radioactivity was counted by a liquid scintillation analyzer (Tri-Carb 2100 TR; Canberra Packard, Schwadorf, Austria[b]). An internal standard (3-[^{3}H]-MVA, specific activity 24.0 mCi/mmol; GE Healthcare) was added to calculate the recovery.

Membrane and lysate preparation

Total membrane and total lysate were obtained as follows: 100 mg skeletal muscle tissue was homogenized in 0.01 M Tris-HCl, 0.001 M $CaCl_2$, 0.15 M NaCl, and 0.001 M PMSF (pH 7.5). An aliquot of homogenate was collected and used for lysate preparation. The remaining homogenate was centrifuged for 20 min at 10,000 *g*. The supernatant was centrifuged at 100,000 *g* for 45 min, and the pellet was resuspended and centrifuged again at 100,000 *g* for 45 min. The pellet was solubilized in 0.125 M Tris-HCl (pH 6.8) containing 10% SDS and protease inhibitor cocktail (sample buffer) and transferred into microtubes. The aliquot of homogenate was solubilized by sonication in sample buffer and centrifuged for 5 min at 15,600 g, and the supernatant was transferred into microtubes. Protein concentration was determined by the method of Lowry *et al.* (11). All samples were boiled for 3 min before loading for Western blotting.

Protein analysis

Protein profiles were analyzed by Western blotting. Western blot analysis of LDLr and RhoA were performed on total gastrocnemius and EDL plasma membranes, respectively, while the analysis of MHC isoforms, poly(ADP-ribose) polymerase-1 (PARP-1), AMPKα, and Akt were performed on total EDL lysates. Protein (20 μg) from solubilized membranes was resolved by 12% (for RhoA), 10% (for P-Akt, total Akt, P-AMPKα, and total AMPKα), and 7% (for LDLr, MHC isoforms, and PARP-1) SDS-PAGE at 100 V for 60 min. SDS-PAGE for MHC isoforms was performed at 140 V for 6 h at 4°C. The proteins were subsequently transferred electrophoretically onto nitrocellulose for 90 min at 100 V. The nitrocellulose membrane was blocked at room temperature with 5% fat-free milk in Tris-buffered saline (138 mM NaCl, 27 mM KCl, 25 mM Tris–HCl, and 0.05% Tween-20, pH 6.8), and probed at 4°C overnight with primary antibodies (RhoA 26C4 and PARP-1 F-2, Santa Cruz Biotechnology, Santa Cruz, CA, USA; LDLr ab30532, Abcam, Cambridge, UK; fast MHC MY-32, slow MHC NOQ7.5.4D, Sigma; P-AMPKα, total AMPKα, P-Akt, and Akt, Cell Signaling, Danvers, MA, USA) followed by incubation for 1 h with secondary IgG antibodies coupled to horseradish peroxidase (Bio-Rad Laboratories, Milan, Italy). The nitrocellulose membrane was then stripped with Restore Western blot stripping buffer (Pierce Chemical, Rockford, IL, USA) for 10 min at room temperature and reprobed with anti-tubulin (α-tubulin DM-1A; Sigma) or anti-caveolin (caveolin-1 N-20; Santa Cruz Biotechnology) antibodies. Bound antibodies were visualized using enhanced chemoluminescence detection (GE Healthcare). All images derived from Western blotting were analyzed with ImageJ (National Institutes of Health, Bethesda, MD, USA) software for Windows. Each reported value was derived from the ratio between arbitrary units obtained by the protein band and the respective tubulin or caveolin band (chosen as housekeeping proteins).

Lipid extraction

EDL muscle (~100 mg) was homogenized in NaCl (150 mM; 1:9, w/v); 6 nmol coenzyme Q6 (CoQ6), 600 μl water, 4 ml methanol, and 4 ml chloroform were added to homogenate. CoQ6 was added as internal standard to calculate the recovery. The samples were incubated for 30 min at 37°C. Then, 800 μl NaCl 150mM and 2 ml chloroform were added, and 2 phases were obtained. The lower phase was evaporated with a stream of nitrogen. Samples were dissolved in 0.5 ml chloroform and then divided into halves. The samples used to measure CoQ9 amount were dissolved in 50 μl isopropanol:ethanol (1:1, v/v); the samples employed to estimate cholesterol and dolichol levels were hydrolyzed in 0.5 ml 15% KOH in ethanol:water (95:5, v/v) for 60 min at 95°C. Then the organic phase was extracted with 0.5 ml of water and 1 ml of hexane. The upper phase was collected and evaporated with a stream of nitrogen, then dissolved in 50 μl isopropanol:ethanol (1:1, v/v).

HPLC-UV analysis of polyisoprenoids

Lipids were analyzed according to previously described protocol (12) with modifications. Briefly, two parallel runs, one for CoQ9 and another for cholesterol, were performed on a 4.6- × 75-mm Zorbax XDB-C18 (3.5 μm) reversed-phase column (Agilent, Santa Clara, CA, USA) using a Waters dual-pump apparatus, a Waters gradient programmer, and a Waters photodiode array detector (spectrum range: 210–400 nm; Waters Corp., Milford, MA, USA). For elution, a combination of convex gradients (Waters No. 5, from 0 to 75% B for the initial 20 min and linear, from 75 to 100% B during the following 10 min) was used; in the last 5 min, reequilibration back to 0% B was performed, where solvent A was methanol: water (9:1, v/v), and solvent B was methanol:propan-2-ol/hexane (2:1:1, v/v/v). The solvent flow rate was 1.5 ml/min. HPLC solvents were obtained from POCh (Gliwice, Poland). The chain length and identity of lipids were confirmed by applying following standards: CoQ_6, CoQ_{10}, and cholesterol. CoQ_{10} and cholesterol were purchased from Sigma-Aldrich; CoQ_6 was from the Collection of Polyprenols (Institute of Biochemistry and Biophysics, PAS, Warsaw, Poland).

Morphological analysis

Fixed EDL muscles were dehydrated in graded ethanol, transferred to Bioclear (BioOptica, Milan, Italy) and then to a 1:1 mixture of Bioclear and paraffin, and finally embedded in paraffin. Transverse, 7-μm-thick sections were cut by a microtome and collected on Vectabond precoated slides (Vector, Burlingame, CA, USA). Sections were deparaffinized, rehydrated, and submitted to antigen retrieval, using antigen unmasking solution (Vector). After cooling, slides were transferred to PBS containing 3% hydrogen peroxide, for 5 min, in the dark, then to PBS with 0.2% Triton X-100 and 3% bovine serum albumin (BSA), for 1 h at room temperature. Sections were incubated overnight at 4°C with either of the following mouse polyclonal antibodies, diluted in PBS containing 0.1% Triton X-100 and 1.5% BSA: fast MHC MY-32 1:1000, slow MHC NOQ7.5.4D 1:5000 (Sigma). In control sections, the primary antibody was omitted. Slides were then incubated for 1 h at room temperature with biotinylated goat anti-rabbit IgG (Vector), diluted 1:200 in PBS containing 1% normal goat serum (Vector). Immunocomplexes were revealed by means of an avidin biotin system (Vectastain Elite ABC kit, Vector), using 3,3′-diamino-benzidine (DAB Substrate kit for peroxidase; Vector), as the chromogen. Sections were counterstained with hematoxylin, then dehydrated and mounted with Eukitt (Kindler GmbH & Co., Freiburg, Germany). Slides were observed under an Olympus BX 51 microscope (Olympus, Tokyo, Japan) equipped with a Leica DFC 420 camera (Leica Microsystems, Wetzlar, Germany); electronic images were captured by a Leica Application Suite system, and composed in an Adobe Photoshop CS2 format (Adobe Systems, San Jose, CA, USA).

Mechanical analysis

EDL muscle was dissected by using scissors and forceps under a stereomicroscope (Stemi SV11; Carl Zeiss MicroImaging, Oberkochen, Germany) and mounted horizontally, between the lever of a motor/force transducer system (305C, Aurora Scientific Inc., Aurora, ON, Canada) and a lever carried by a micromanipulator, in a trough, containing physiological solution (Krebs-Henseleit solution, composition, in mM: 119 NaCl, 4.7 KCl, 2.5 $CaCl_2$, 1.0 $MgSO_4$, 25 $NaHCO_3$, 1.2 KH_2PO_4, and 1.1 glucose) gassed with carbogen (95% O_2 and 5% CO_2, pH7.4). The muscle was straightened just above its slack length by means of the micromanipulator. The trough was sealed with a Perspex cover and mounted vertically on the stage with the motor/force transducer system on top. The solution was continuously saturated with carbogen during the experiment. Room temperature was in the range 20–22°C.

Trains of stimuli of alternate polarity to elicit fused tetani (frequency 70–80 Hz) were delivered by means of two platinum wire electrodes running parallel to the muscle, 1 cm apart. The intensity of the stimuli was increased until the isometric plateau force reached a maximum constant value T_0 (indicating that all the cells in the muscle were activated). The muscle length was finely adjusted further by means of the micromanipulator to obtain the maximum isometric force,

corresponding to the plateau of the force-length relation. To compare isometric force among muscles, the isometric plateau force was normalized by the wet weight of the muscle, measured at the end of each experiment with an electrobalance (CP124S; Sartorius, Goettingen, Germany). The force-velocity relation was determined by measuring the velocity of steady shortening V after a drop in force from the isometric value T_0 to a preset value $T<T_0$. The force-velocity points were fitted to the Hill hyperbolic equation (Eq. 1):

$$(T + a) \cdot (V + b) = (V_0 + b) \cdot a \quad (1)$$

where a, b, and V_0 (the unloaded shortening velocity) are the regression parameters.

To investigate the effects of simvastatin on muscle endurance, a fatiguing protocol was used. EDL muscle was given a 400-ms fused tetanus every 3 s over a period of 150 s. The muscle was then allowed to recover for a period of 40 min, during which force recovery was monitored with a tetanus every 5 min. Force, length change, and stimulus were recorded with a multifunction I/O board (PCI-6110E; National Instruments, Austin, TX, USA) at 0.5-ms sampling rate. A program written in LabVIEW (National Instruments) was used for signal recording and analysis.

Functional analysis

Rotarod motor coordination test

To assess any effect of simvastatin on motor coordination and balance, rats were tested in an automated accelerating rotarod apparatus (Biological Research Apparatus; Ugo Basile, Varese, Italy; ref. 13). The apparatus consisted of 7-cm-diameter plastic drums machined with grooves to improve grip, that could be set on accelerating speed (4, 10, 12, 15, 19, 22, 26, 29 34 and 40 rpm, 30 s at each speed).

Before testing, the rats were trained for 2 d, applying the following schedule (14): the first day, the rats were trained for 3 min with an unlimited number of trials on the rotarod, followed by 4 trials of maximum 60 s with a 30 s intertrial interval; the second day, the rats were placed on the rotarod at accelerating speed for a maximum of 300 s. Testing was performed after 21 d of treatment with simvastatin; each rat was individually placed on the rotarod at accelerating speed for a maximum of 300 s, and the latency to fall off the rotarod and the maximum speed reached within this time period were recorded. Immediately after each session, the apparatus was thoroughly cleaned with cotton pads wetted with 70% ethanol;water solution and dried. Rats were allowed to habituate to the experimental room for 60 min before both training and testing. Training and testing were performed between 10:00 AM and 1:00 PM.

Open-field locomotor activity

The day after rotarod testing, the rats were tested for horizontal locomotor activity. The animals were transferred from the holding room to the experimental room, where they were allowed to habituate for 60 min. Testing was conducted under dim light between 10:00 AM and 1:00 PM. The test started by placing each animal in the center of an open-field arena (80×80 cm) made of gray Plexiglas. Behavior was videorecorded for 10 min using a digital video camera for subsequent analysis. All scores were assigned by the same observer, who was unaware of animal treatment. Immediately after each session, the apparatus was thoroughly cleaned with cotton pads wetted with 70% ethanol:water solution and dried. The following behavioral parameters were scored: number of crossings (crossing with both forepaws the lines in which the floor of the arena was subdivided on the monitor), time spent near the walls (periphery), time spent in the central part of the arena, and frequency and duration of rearing (standing with the body inclined vertically, forequarters raised), wall-rearing (standing on the hind-limbs and touching the walls of the apparatus with the forelimbs), and grooming (rubbing the body with paws or mouth and rubbing the head with paws).

Statistical analysis

Data are expressed as means ± SD. The difference of parameters was statistically tested for significance with unpaired Student's t test. Values of $P < 0.05$ were considered to indicate a significant difference. Statistical analysis was performed using GraphPad Instat3 (GraphPad, Inc., La Jolla, CA, USA) and SigmaPlot (Systat Software Inc., San Jose, CA, USA) for Windows.

RESULTS

Simvastatin efficacy and tolerance

Simvastatin efficacy in lowering plasma LDL-cholesterol (15) and triglycerides (16) by hepatic LDLr up-regulation (17) was verified by checking rat plasma cholesterol and triglyceride content (**Table 1**). As expected, both the metabolic parameters decreased significantly with the following treatment, by 30% and 53%, respectively. Nevertheless, simvastatin treatment did not modify animal weight, even though the weight of treated animals was slightly lower than that of rats receiving vehicle (**Fig. 1*A***). Moreover, simvastatin treatment lowered HMGR activity in the gastrocnemius muscle by 20% (Fig. 1*B*). Evidence for drug efficacy on skeletal muscle was also given by the increased levels of LDLr protein in the gastrocnemius muscle of treated rats (Fig. 1*C*), in good agreement with the rise of LDLr mRNA observed previously (18).

Once simvastatin efficacy on skeletal muscle was ascertained, our attention focused on the effects exerted by HMGR inhibition on EDL muscle, which consists mainly of fast and glycolitic fibers, given that the glycolitic fibers appear to be the most susceptible to statin side effects (19). Thus, the levels of HMGR end products involved in skeletal muscle contraction, such as CoQ9 (4), cholesterol (3), and a prelynated protein

TABLE 1. *Effect of simvastatin on metabolism of treated and control rats*

Component	Vehicle	Simvastatin, 1.5 mg/kg	P
Cholesterol (mg/dl plasma)	82.35 ± 9.45	57.52 ± 9.22	<0.01
Triglycerides (mg/dl plasma)	189.6 ± 37.71	88.86 ± 30.48	<0.001

Seven rats contributed to each value. Statistical analysis was done by unpaired t test.

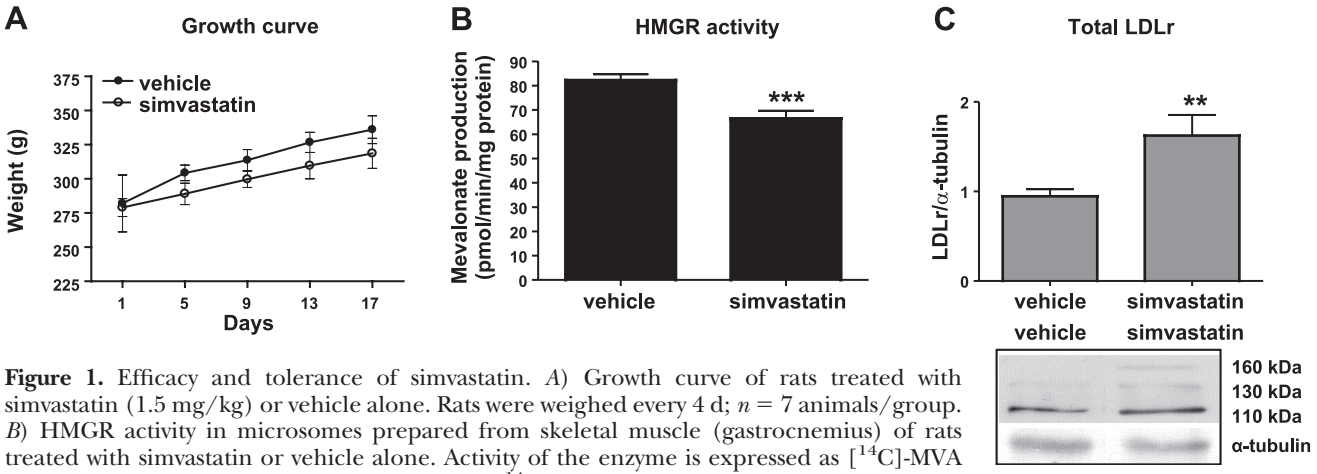

Figure 1. Efficacy and tolerance of simvastatin. *A*) Growth curve of rats treated with simvastatin (1.5 mg/kg) or vehicle alone. Rats were weighed every 4 d; $n = 7$ animals/group. *B*) HMGR activity in microsomes prepared from skeletal muscle (gastrocnemius) of rats treated with simvastatin or vehicle alone. Activity of the enzyme is expressed as [^{14}C]-MVA production (pmol/min/mg protein) from 3-[^{14}C]-HMG CoA added to the samples. *C*) Representative Western blot (bottom panel) and densitometric analysis (top panel) of LDLr protein levels. The 3 bands (110, 130, 160 kDa) detected represent the different and increasing glycosylation state of the LDLr. Protein levels were normalized to α-tubulin content. Data are expressed as arbitrary units; $n = 7$ animals/group. Values are presented as means ± SD. $^{**}P < 0.01$, $^{***}P < 0.001$; Student's *t* test.

(RhoA) (5, 20), were assessed. As shown in **Table 2**, no significant differences were detected in EDL muscles of simvastatin-treated rats either in cholesterol or in CoQ9 content. In addition, as shown in **Fig. 2*A***, the translocation of RhoA on EDL plasma membrane and its consequent activation (21) did not differ in simvastatin-treated animals when compared to controls.

Effects of simvastatin treatment on muscular damage

To ascertain whether the pharmacological treatment could have caused possible muscle damage, as described previously (2, 8), plasma CKs (22), and muscle cleaved PARP-1 protein levels, markers for muscle fiber necrosis and apoptosis, respectively, were checked (Fig. 2*B, C*). Both CK and PARP-1 protein levels were not increased in simvastatin treated rats with respect to the control showing the absence of muscle fiber necrosis and/or apoptosis.

MHC isoform determination

Previous data demonstrated that HMGR inhibition by mevinolin (3 μM) can modulate fetal MHC expression in L6 myoblasts (9). This finding prompted us to assess whether a putative modification of MHC isoform expression could occur in EDL muscle after simvastatin treatment. Morphological observation of sections from simvastatin-treated EDL muscles indicated unaltered cytoarchitecture, compared to controls. The immunohistochemical localization of fast and slow MHC isoforms on EDL muscles from simvastatin-treated and control rats showed similar, though not identical, distribution of positive fibers in either conditions (**Fig. 3**). Muscle cells immunoreactive to anti-fast MHC isoform represented the large majority of fibers in sections from both treated and untreated muscles (Fig. 3*A, B*). However, the occurrence of negative fibers, most probably corresponding to slow MHC isoform-expressing cells, appeared to be increased after treatment. Accordingly, simvastatin seemed to produce an increased frequency of slow MHC immunoreactive fibers, as shown in Fig. 3*C, D*, but the data are not statistically significant. Moreover, an enhanced immunodensity of the positive cells was detected after the pharmacological treatment, suggesting that the expression of slow MHC isoform could be higher under this condition.

Immunohistochemical analysis suggests that a change in fiber structure could occur. To better ascertain putative differences in MHC isoform expression, Western blot analysis was performed. As observed in **Fig. 4*A***, no differences were detected in the slow MHC isoform expression. The apparent discrepancy between the data obtained by immunohistochemistry and those obtained by Western blot can be explained if the low percentage of EDL fibers expressing the slow MHC isoform is considered. Thus, Western blot analysis is not sensitive enough to detect the difference highlighted through morphological observation. Electrophoresis separation shows a shift of the fast MHC isoforms, from the fastest

TABLE 2. *Effect of simvastatin treatment on HMGR end products of the mevalonate pathway*

End product	Vehicle	Simvastatin, 1.5 mg/kg	*P*
Cholesterol (μg/g tissue)	92.10 ± 10.94	106.56 ± 10.87	0.22
CoQ9 (μg/g tissue)	19.09 ± 8.04	17.43 ± 5.63	0.84

Seven muscles contributed to each value. Statistical analysis was done by unpaired *t* test.

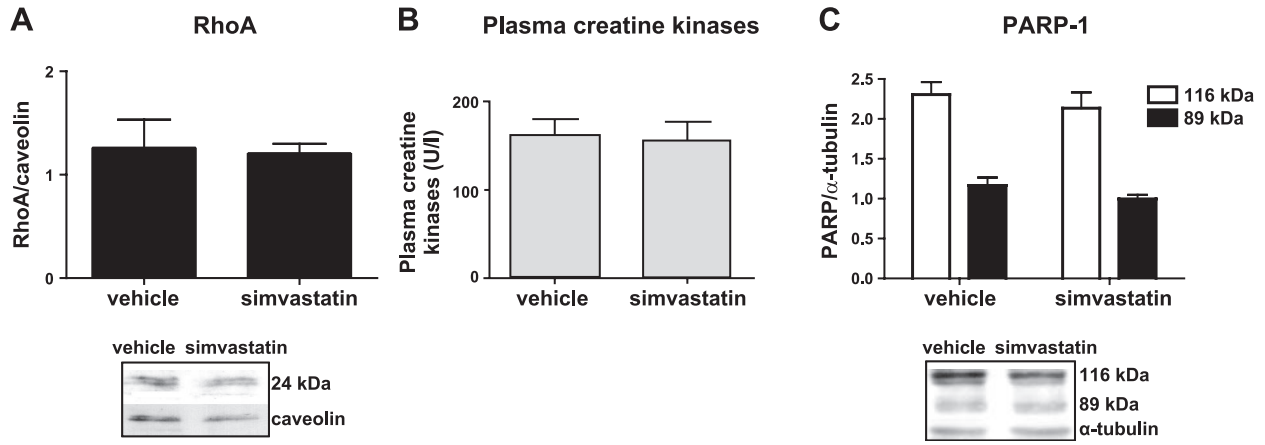

Figure 2. Biochemical measurements on simvastatin-treated and control rats. *A*) RhoA levels in EDL membranes of simvastatin-treated and control rats. Representative Western blot (bottom panel) and densitometric analysis (top panel) of RhoA detected in total membranes prepared from EDL muscle of rats treated with simvastatin or vehicle alone. Protein levels were normalized to caveolin content. Data are expressed as arbitrary units; $n = 7$ animals/group. *B*) Creatine kinase levels (U/L) detected from plasma of rats treated with simvastatin or vehicle alone. *C*) Representative Western blot (bottom panel) and densitometric analysis (top panel) of full-length (116 kDa) and cleaved (89 kDa) PARP-1 detected in total lysates obtained from EDL muscle of rats treated with simvastatin or vehicle alone. Protein levels were normalized to α-tubulin content. Data are expressed as arbitrary units; $n = 7$ animals/group. Values are presented as means ± SD.

MHC IIb to the slower MHC IIa/x (Fig. 4*B*) in the simvastatin-treated rats with respect to control. In the control group, EDL muscle contained ~85% of MHC IIb isoform, with a small (15%) amount of MHC IIa/x isoforms, while EDL muscle of simvastatin-treated rats contained ~70% of MHC IIb isoform, and 30% of MHC IIa/x isoforms.

Statin treatment can interfere with the intracellular pathways responsible for MHC isoform switch; thus, the activity of Akt and of AMPK, whose phosphorylation states were demonstrated to be modified by statins (23, 24), was analyzed. In particular, Akt and AMPK are negative and positive regulators, respectively, of peroxisome proliferator-activated receptor-γ coactivator 1-α (PGC-1α), which plays a central role in muscle plasticity (25). **Figure 5** shows that no changes in the phosphorylation levels of these two kinases are observable after simvastatin treatment.

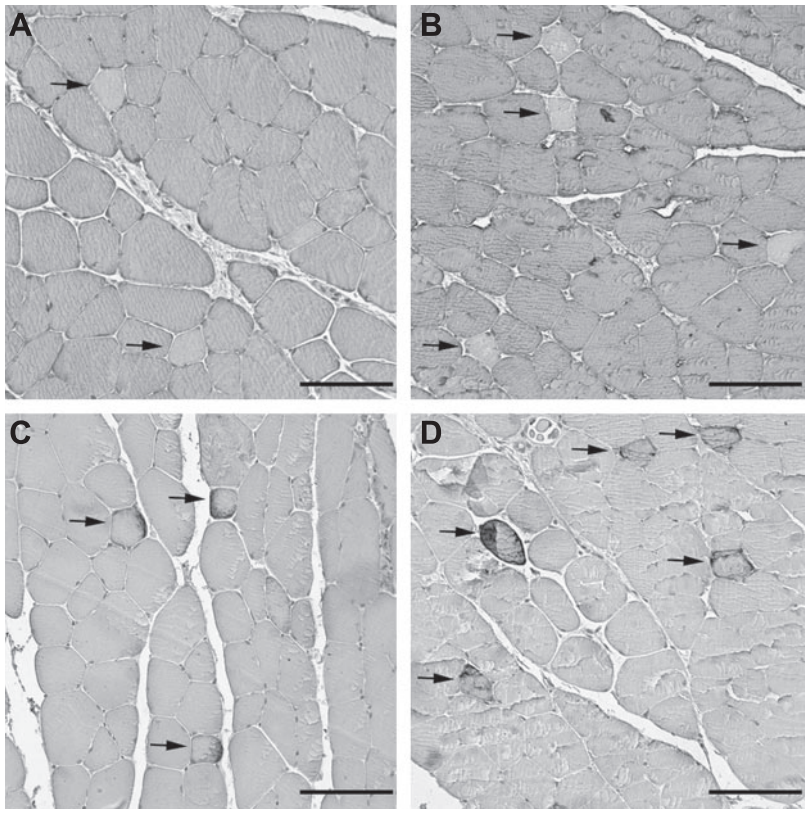

Figure 3. Immunohistochemical localization of fast and slow MHC isoforms in EDL muscle sections from simvastatin-treated and control rats. *A, B*) Fast MHC isoform immunohistochemistry in control (*A*) and simvastatin-treated (*B*) EDL muscle sections. Positive fibers are widely distributed in the tissue, under both conditions. However, immunonegative cells (arrows) are more numerous in simvastatin-treated muscle, compared to control. *C, D*) Slow MHC isoform immunohistochemistry in control (*C*) and simvastatin-treated (*D*) EDL muscle sections. Scattered, positive fibers are observed in the tissue, under both conditions. However, higher numbers of positive cells (arrows), showing intense immunoreactivity, are present in treated muscle, compared to control. Scale bars = 100 μm.

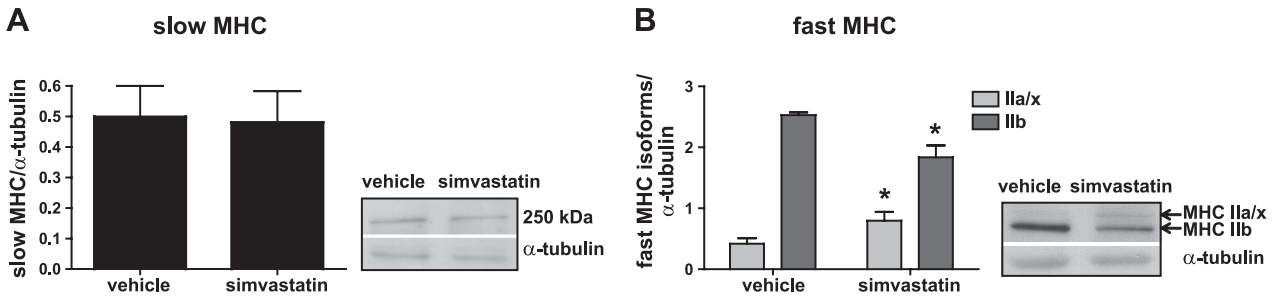

Figure 4. Slow and fast MHC protein levels in EDL muscle of simvastatin-treated and control rats. *A*) Typical Western blot (right panel) and densitometric analysis (left panel) of slow MHC detected in total lysates prepared from EDL muscle of rats treated with simvastatin or vehicle alone. *B*) Representative Western blot (right panel) and densitometric analysis (left panel) of fast MHC detected in total lysates prepared from EDL muscle of rats treated with simvastatin or vehicle alone. Protein levels were normalized to α-tubulin content. Data are expressed as arbitrary units; $n = 7$ animals/group. Values are presented as means ± SD. $^*P < 0.05$; Student's t test.

Effect of simvastatin treatment on muscle function

To understand whether the observed shift from the fastest MHC IIb isoform to the slower MHC IIa/x isoforms could affect the mechanical properties of EDL muscle, the effects of simvastatin treatment on the contractile properties of fast skeletal muscle were evaluated. In particular, the maximum steady force elicited by the isometric tetanus T_0, twitch-to-tetanus ratio t/T_0, time to attain half of the isometric tetanic plateau force $t_{1/2}$, and force-velocity relation (**Table 3** and **Fig. 6**) were recorded. T_0 was normalized by the different mass of muscles by mean of the procedure described in Materials and Methods. Simvastatin treatment, with respect to control, reduced T_0 and t/T_0 by 23 and 22%, respectively (but the difference is not statistically significant; Table 3); significantly increased $t_{1/2}$ by 25% (Table 3); and reduced the shortening velocity at any load below T_0 (Fig. 6*C* and Table 3). Consequently, the power, calculated as the product $T \cdot V$, was significantly reduced in simvastatin-treated rats (Fig. 6*D*). At the load for the maximum power, ~0.3 T_0, the power (W_{max}) was 41% lower in simvastatin-treated than in control rats (Table 3). The unloaded shortening velocity V_0, estimated as parameter of the Hill hyperbolic equation (Eq. 1), was 23% lower in simvastatin-treated than in control rats (Table 3). To investigate whether simvastatin treatment affects not only power but also endurance, EDL muscles were subjected to a fatigue protocol (see Materials and Methods). Results showed no difference in the time course of isometric force reduction to get 40% of the prefatigue value (**Fig. 7**), indicating that endurance performance is not affected by simvastatin treatment. Also, the time course of force recovery from fatigue, over 40 min from the end of the fatigue protocol, which allows isometric force to recover ~30% of force decay in control, showed no effect of simvastatin treatment (ascending part of the curves in Fig. 7).

Rotarod motor coordination and open-field locomotor activity tests

To assess further whether the effects of simvastatin on skeletal muscle could result in functional impairments, we tested the effect of this treatment regimen on motor coordination and locomotor activity in rats. Treatment with simvastatin impaired performance in the rotarod test. Indeed, simvastatin-treated rats showed reduced latency to fall off the rotarod and reduced maximum speed reached during test compared to vehicle-treated animals (**Fig. 8**). Simvastatin-treated rats did not differ from vehicle-treated rats for any parameter measured in the open-field test (number of crossings, **Fig. 9*A***;

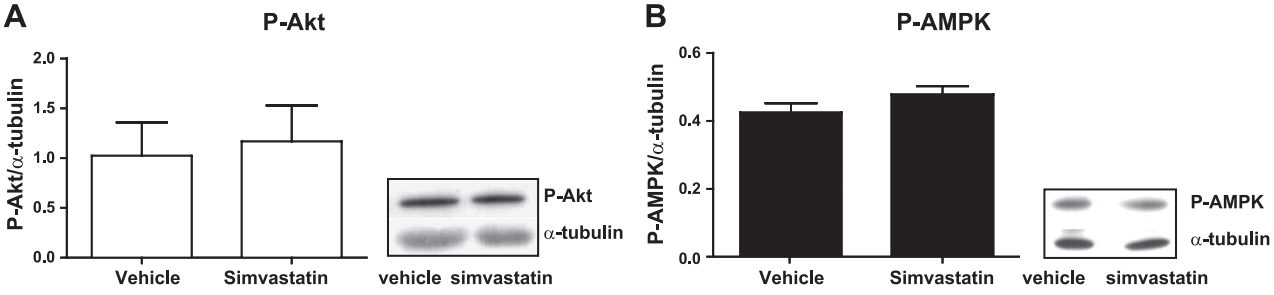

Figure 5. P-Akt and P-AMPK protein levels of simvastatin-treated and control rats. *A*) Typical Western blot (right panel) and densitometric analysis (left panel) of P-Akt detected in total lysates prepared from EDL muscle of rats treated with simvastatin or vehicle alone. *B)* Typical Western blot (right panel) and densitometric analysis (left panel) of P-AMPK detected in total lysates prepared from EDL muscle of rats treated with simvastatin or vehicle alone. Protein levels were normalized to α-tubulin content. Data are expressed as arbitrary units; $n = 7$ animals/group. Values are presented as means ± SD.

TABLE 3. *Effect of simvastatin treatment on mechanical parameters during isometric contraction and isotonic shortening of EDL muscle*

Parameter	Vehicle	Simvastatin, 1.5 mg/kg	*P*
Isometric contraction			
L_0 (cm)	2.96 ± 0.06	2.90 ± 0.17	0.56
w (g)	0.157 ± 0.020	0.164 ± 0.015	0.85
CSA (cm^2)	0.110 ± 0.013	0.134 ± 0.021	0.88
T_0 (N/g)	13.49 ± 1.25	10.33 ± 5.26	0.21
t/T_0	0.325 ± 0.043	0.254 ± 0.019	0.06
$t_{1/2}$ (ms)	22.9 ± 3.5	28.7 ± 6.7	<0.01
Isotonic shortening			
V_0 (L_0/s)	3.87 ± 0.13	2.98 ± 0.14	<0.01
a/T_0	2.78 ± 0.31	2.42 ± 0.40	0.47
b (L_0/s)	2.14 ± 0.29	2.00 ± 0.37	0.77
W_{max} (mW/g)	134.7 ± 11.3	79.7 ± 3.4	<0.01

Four muscles contributed to each value. Statistical analysis was done by unpaired t test. Isometric contraction parameters: L_0, muscle length at the plateau of the force-length relation; w, muscle wet weight; CSA, cross-sectional area of muscle, calculated using the relation CSA = $w/(L_0*k*\delta)$ (cm^2), where δ is the density of the muscle (1.056 g/cm^3) and k is a constant (0.40 for EDL muscle; ref. 39); T_0, isometric force; t/T_0, twitch-to-tetanus ratio; $t_{1/2}$, time to attain half of the tetanic isometric force. Isotonic shortening parameters: V_0, a/T_0, and b are regression parameters of the Hill hyperbolic equation (Eq. 1) fitted to the pooled data for simvastatin-treated rats and control, with statistical analysis by Student's t test of difference of means; W_{max}, maximum power, obtained with a load ~1/3 the isometric force.

time in periphery, Fig. 9*B*; time in center, Fig. 8*C*; data not shown for frequency and duration of wall-rearing, rearing, and grooming).

DISCUSSION

In the current study, we investigated the role of HMGR inhibition by simvastatin on skeletal muscle physiology. This lipophilic HMGR inhibitor was chosen because the lipophilic statins are generally taken up much more widely into a broad range of tissues and cells by diffusion compared with hydrophilic statins (26). Chronic treatment with simvastatin (1.5 mg/kg) inhibits HMGR activity in skeletal muscle to a similar extent as in the liver, where the effect of statins is well documented (19); induces a shift of MHC isoforms toward a slower phenotype; reduces the power output and the unloaded shortening velocity of EDL muscle without a significant reduction in isometric force and resistance to fatigue; and induces functional impairment, *i.e.*, reduction in the latency to fall off the rotarod.

Because power involves not just force production but also the speed at which the force is produced, deficits in muscle power can be related to impairment in movement

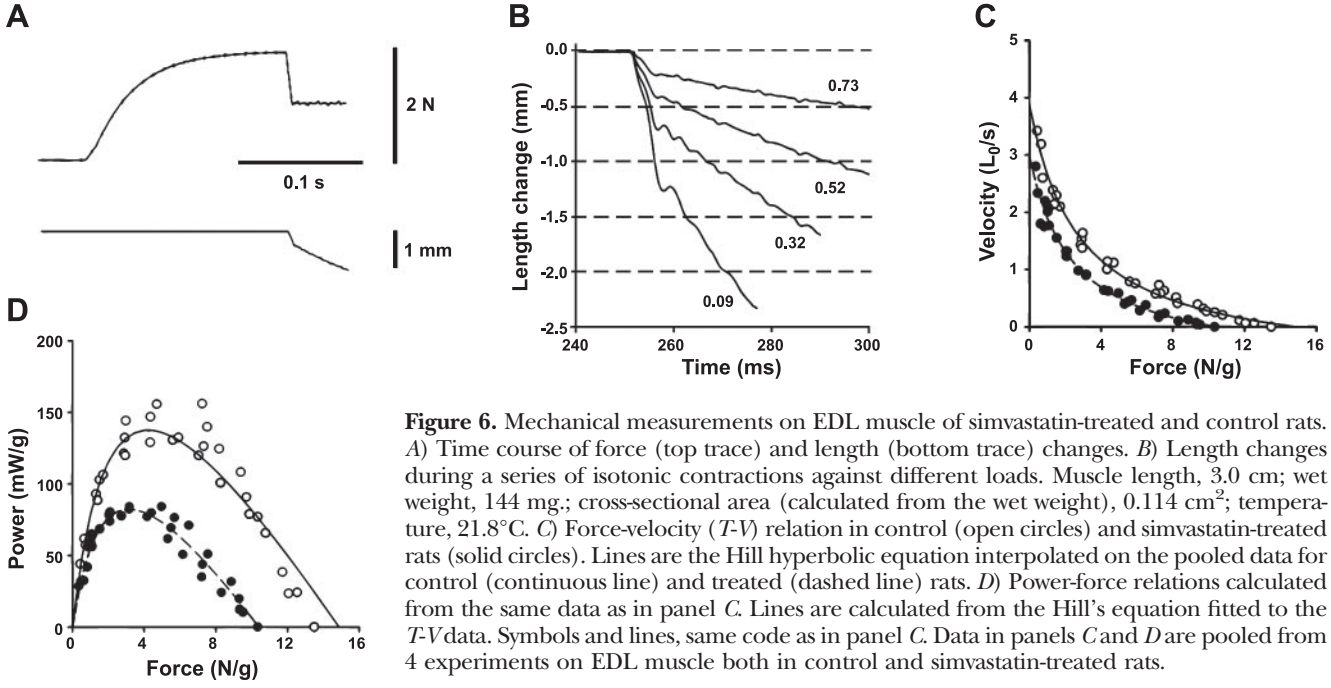

Figure 6. Mechanical measurements on EDL muscle of simvastatin-treated and control rats. *A*) Time course of force (top trace) and length (bottom trace) changes. *B*) Length changes during a series of isotonic contractions against different loads. Muscle length, 3.0 cm; wet weight, 144 mg.; cross-sectional area (calculated from the wet weight), 0.114 cm^2; temperature, 21.8°C. *C*) Force-velocity (*T-V*) relation in control (open circles) and simvastatin-treated rats (solid circles). Lines are the Hill hyperbolic equation interpolated on the pooled data for control (continuous line) and treated (dashed line) rats. *D*) Power-force relations calculated from the same data as in panel *C*. Lines are calculated from the Hill's equation fitted to the *T-V* data. Symbols and lines, same code as in panel *C*. Data in panels *C* and *D* are pooled from 4 experiments on EDL muscle both in control and simvastatin-treated rats.

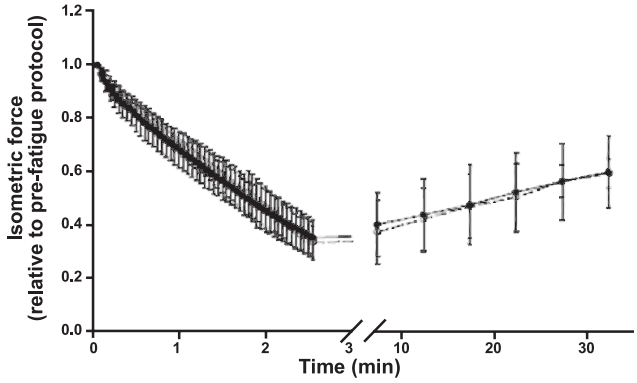

Figure 7. Effects of simvastatin on muscle endurance. Changes in isometric force on EDL muscle in simvastatin-treated (solid circles) and control rats (open circles) during fatigue and recovery. EDL muscles were subjected to a fatigue protocol consisting of a 400-ms, 100-Hz tetanus every 3 s for 150 s. Descending part of the curve shows the decline in isometric force. Ascending part of the curve shows the partial recovery of isometric force up to 40 min from the end of the fatigue protocol. $n = 4$/group. Data are means ± SD.

and locomotion (27, 28). Biochemical analysis shows that simvastatin treatment, by means of the shift toward a slower MHC isoform phenotype, reduces EDL muscle functions without exerting any muscle damage, in agreement with the lack of evidence for reduction in isometric force.

The drug efficacy on skeletal muscle tissue was ascertained by determining HMGR activity and LDLr protein levels. In agreement with previous studies in hepatocytes, simvastatin inhibits HMGR activity and increases the expression of LDLr (19). The putative myotoxic effects of the drug, whose underlying mechanisms are still debated, were excluded by the analysis of muscle damage markers. It is known that statin administration can induce muscle fiber necrosis, with release of cellular constituents such as CK into the bloodstream (2), and a caspase-dependent apoptotic cascade leading to the PARP-1 cleavage (29). Any significant increase of plasma CK and cleaved PARP-1 protein levels in simvastatin-treated rats was found, indicating that, in agreement with the lack of evidence for reduction in isometric force, the reduced muscle function is not related to muscle fiber loss due to apoptosis or necrosis. The absence of muscle damage could be explained by the lower dose of simvastatin used in our study, 1.5 mg/kg (comparable to the highest dose used to treat hypercholesterolemia in the clinical practice), with respect to the doses used in previous studies where muscle damages were described (30). In fact, the maximum simvastatin dose administered in clinical practice is 80 mg/d, corresponding, on average, to 1.14 mg/kg/d; since the metabolism rate of rats is higher than that of humans, the dose administered to the animals was slightly increased. We also excluded that the impairment of EDL muscle function was due to modified levels of HMGR end products directly involved in muscle contraction; neither cholesterol nor CoQ9 changed significantly in treated animals. However, this result cannot rule out a modulation of HMGR main end products by simvastatin, since only 50% of the body CoQ9 is derived from endogenous synthesis through the MVA pathway, and the remaining 50% is thought to be obtained through fat ingestion (4) and carried mainly by LDL in the circulation (12). Thus, like cholesterol, putative CoQ9 depletion due to enzyme inhibition by simvastatin could have been restored within the cells and, in turn, within the tissues by an enhanced LDLr-mediated uptake, as suggested by the increased LDLr protein expression. Furthermore, the levels of RhoA were evaluated both because the post-translational modification with a prenyl group (an HMGR product) is necessary for its membrane association and consequent activation, and because RhoA can activate Rho-kinase, responsible for MLC phosphorylation and, in turn, involved in the regulation of muscle contraction. Nevertheless, RhoA activation state did not change in either animal group.

Morphological but overall biochemical analysis show a change of sarcomeric proteins belonging to the contractile machinery of the muscle toward a slower phenotype, especially in the MHC composition of the fibers within the muscle, which leads to the reduced muscle function (31, 32). Specifically, simvastatin treatment induces a shift from the fastest MHC IIb isoform to the slower MHC IIa/x isoforms. The amount of reduction of V_0 (23%), W_{max} (41%), and $t_{1/2}$ (25%), as well as the lack of significant change in T_0, are in qualitatively good agreement with the changes of these parameters described in muscles and in fully Ca^{2+}-activated skinned fibers from fast skeletal muscles of mammalians containing different MHC isoforms (31–35). In particular, fast fibers from rats containing pure MHC IIa isoform have V_0 ~30% lower than those containing MHC IIx isoform, and the latter have V_0 ~20% lower than fibers containing MHC IIb isoform, while the maximum power in fibers containing MHC IIa/x isoforms is 30–60% lower than in fibers containing MHC IIb isoform (33). Moreover, the endurance of EDL muscle, determined by a fatigue protocol, is not affected by simvastatin.

The simvastatin-induced impairment of muscle performance was also supported by an *in vivo* functional test. These changes resulted in reduced maximum speed reached and reduced latency to fall off the accelerating rotarod in the absence of general impair-

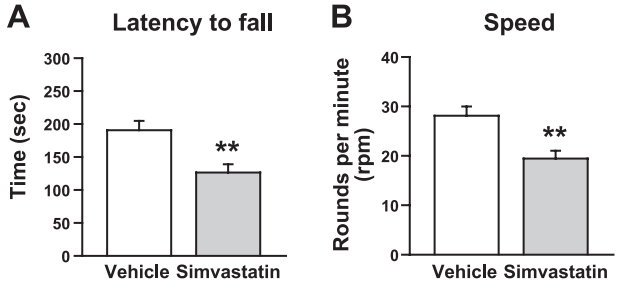

Figure 8. Effects of simvastatin in the rotarod test. Simvastatin-treated rats showed reduced latency to fall off the rotarod (t=3.35, df=17, P<0.01; *A*) and reduced maximum speed reached during the test (t=3.48, df=17, P<0.01; *B*). n = 10/group. $^{**}P < 0.01$; Student's t test.

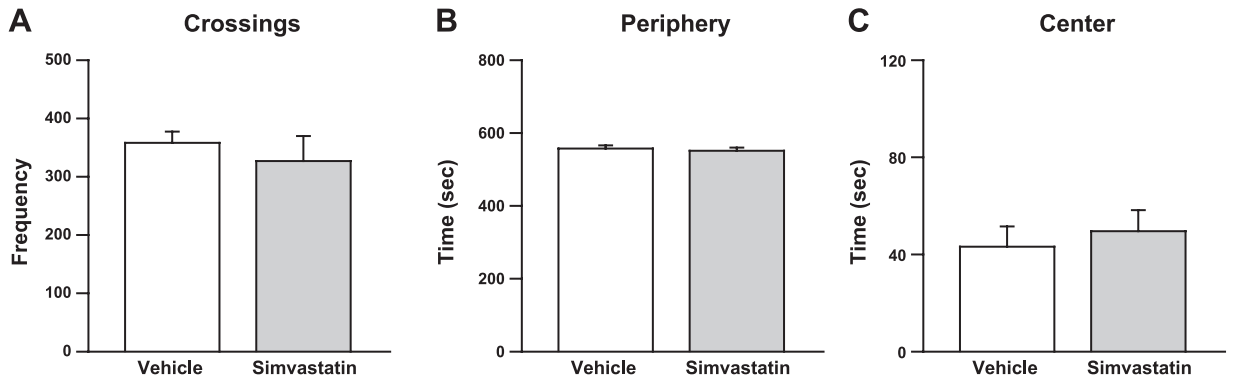

Figure 9. Effects of simvastatin in the open-field test. Simvastatin-treated rats did not differ from vehicle-treated rats in the number of crossings (t=0.67, df=17, n.s.; *A*) and in the time spent both in periphery (t=0.51, df=17, n.s.; *B*) and in center (t=−0.53, df=17, n.s.; *C*). Moreover, simvastatin- and vehicle-treated rats did not differ in frequency and duration of wall-rearing, rearing, and grooming (data not shown); n = 10/group.

ments in basal locomotor activity, as measured in the open-field test. Thus, simvastatin-treated rats showed normal coordination and were still able to run on the rotarod at low speeds but, compared to vehicle-treated animals, could not run the rod at high speeds.

Our results indicate that the simvastatin-induced impairment of muscle function is not related either to changes in Akt and AMPK phosphorylation or to changes in HMGR end products directly involved in muscle contraction, suggesting that a putative modification of other MVA pathway downstream compounds, such as prenylated proteins (*i.e.*, Cdc42, Ras, Rac) not evaluated in this work could be at the root of the observed phenomena (**Fig. 10**).

Further investigations must define the molecular mechanisms responsible for the fast MHC isoform plasticity. This work establishes that a shift in the fast MHC isoforms is involved in muscle contraction impairment following statin treatment. The observed fast MHC isoform shift could be responsible for the reduced muscle activity, at least in fast muscle, and functional impairment described in statin-treated pa-

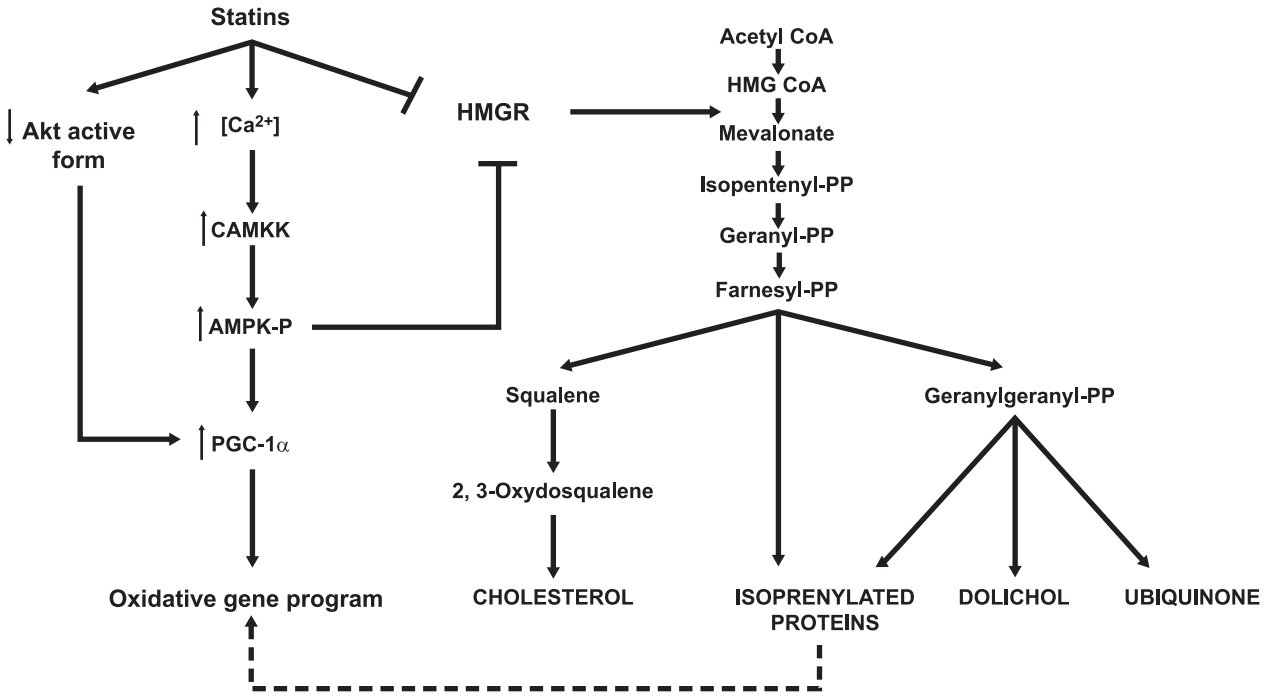

Figure 10. Possible mechanisms responsible for the shift of the fast MHC isofoms in EDL muscle fibers. Simvastatin competitively inhibits the enzyme HMGR (37); can increase the intracellular Ca^{2+} concentration (38), which, in turn, causes an increase of AMPK activity (23); and can suppress Akt phosphorylation. Both the activation of AMPK and the suppression of Akt phosphorylation positively modulate PGC-1α, which drives a coordinated conversion to fibers having characteristics of oxidative type I, IIa, and IIx fibers (25). The lack of any modification in both Akt and AMPK phosphorylation and the absence of changes in HMGR main end products (cholesterol, CoQ9, RhoA) found here, exclude their involvement in MHC shift to slower phenotype in our experimental model. The shift could be ascribable to other prenylated proteins involved in intracellular signal transduction pathway (dotted line in the scheme).

tients (4, 36). This finding suggests that alternative pharmacological approaches should be considered in the management of hypercholesterolemia. FJ

The authors thank Prof. Maria Marino and Anna Trentalance (Department of Biology University Roma Tre) and Prof. Vincenzo Lombardi (Department of Evolutionary Biology, University of Florence) for the helpful discussion. The authors also thank Dr. Maria Morena (Department of Physiology and Pharmacology V. Erspamer, University of Rome La Sapienza, Rome, Italy) for helping with behavioral experiments and Mr. Mario Dolfi (Department of Evolutionary Biology, University of Florence) for skilled technical assistance in mechanical experiments.

REFERENCES

1. Viccica, G., Vignali, E., and Marcocci, C. (2007) Role of the cholesterol biosynthetic pathway in osteoblastic differentiation. *J. Endocrinol. Invest.* **30,** 8–12
2. Ogura, T., Tanaka, Y., Nakata, T., Namikawa, T., Kataoka, H., and Ohtsubo, Y. (2007) Simvastatin reduces insulin-like growth factor-1 signaling in differentiating C2C12 mouse myoblast cells in an HMG-CoA reductase inhibition-independent manner. *J. Toxicol. Sci.* **32,** 57–67
3. Draeger, A., Monastyrskaya, K., Mohaupt, M., Hoppeler, H., Savolainen, H., Allemann, C., and Babiychuk, E. B. (2006) Statin therapy induces ultrastructural damage in skeletal muscle in patients without myalgia. *J. Pathol.* **210,** 94–102
4. Thompson, P. D., Clarkson, P., and Karas, R. H. (2003) Statin-associated myopathy. *JAMA* **289,** 1681–1690
5. Van Aelst, L., and D'Souza-Schorey, C. (1997) Rho GTPases and signalling network. *Genes Dev.* **11,** 2295–2322
6. Burda, P., and Aebi, M. (1999) The dolichol pathway of N-linked glycosylation. *Biochim. Biophys. Acta* **1426,** 239–257
7. Espenshade, P. J., and Hughes, A. L. (2007) Regulation of sterol synthesis in eukaryotes. *Annu. Rev. Genet.* **41,** 401–427
8. Dirks, A. J., and Jones, K. M. (2006) Statin-induced apoptosis and skeletal myopathy. *Am. J. Physiol. Cell Physiol.* **291,** C1208–C1212
9. Martini, C., Trapani, L., Narciso, L., Marino, M., Trentalance, A., and Pallottini, V. (2009) 3-hydroxy 3-methylglutaryl coenzyme A reductase increase is essential for rat muscle differentiation. *J. Cell. Physiol.* **220,** 524–530
10. Bruscalupi, G., Leoni, S., Mangiantini, M. T., Minieri, M., Spagnuolo, S., and Trentalance, A. (1985) True uncoupling between cholesterol synthesis and 3-hydroxy-3-methylglutaryl coenzyme A reductase in an early stage of liver regeneration. *Cell. Mol. Biol.* **31,** 365–368
11. Lowry, O. H., Rosebrough, N. J., Farr, A. L., and Randall, R. J. (1951) Protein measurement with the Folin phenol reagent. *J. Biol. Chem.* **193,** 265–275
12. Tang, P. H., Miles, M. V., DeGrauw, A., Hershey, A., and Pesce, A. (2001) HPLC analysis of reduced and oxidized coenzyme Q(10) in human plasma. *Clin. Chem.* **47,** 256–265
13. Carter, R. J., Morton, J., and Dunnett, S. B. (2001) Motor coordination and balance in rodents. *Curr. Protoc. Neurosci.* Chap. 8, Unit 8.12
14. Voss, J., Sanchez, C., Michelsen, S., and Ebert, B. (2003) Rotarod studies in the rat of the GABAA receptor agonist gaboxadol: lack of ethanol potentiation and benzodiazepine cross-tolerance. *Eur. J. Pharmacol.* **482,** 215–222
15. Chao, Y., Chen, J. S., Hunt, V. M., Kuron, G. W., Karkas, J. D., Liou, R., and Alberts, A. W. (1991) Lowering of plasma cholesterol levels in animals by lovastatin and simvastatin. *Eur. J. Clin. Pharmacol.* **40**(Suppl. 1), S11–S14
16. Ginsberg, H. N. (1998) Effects of statins on triglyceride metabolism. *Am. J. Cardiol.* **81,** 32B–35B
17. Brown, M. S., and Goldstein, J. L. (2004) Lowering plasma cholesterol by raising ldl receptors. 1981. *Atheroscler. Suppl.* **5,** 57–59
18. Yokoyama, M., Seo, T., Park, T., Yagyu, H., Hu, Y., Son, N. H., Augustus, A. S., Vikramadithyan, R. K., Ramakrishnan, R., Pulawa, L. K., Eckel, R. H., and Goldberg, I. J. (2007) Effects of lipoprotein lipase and statins on cholesterol uptake into heart and skeletal muscle. *J. Lipid Res.* **48,** 646–655
19. Westwood, F. R., Bigley, A., Randall, K., Marsden, A. M., and Scott, R. C. (2005) Statin-induced muscle necrosis in the rat: distribution, development, and fibre selectivity. *Toxicol. Pathol.* **33,** 246–257
20. Bozzo, C., Stevens, L., Toniolo, L., Mounier, Y., and Reggiani, C. (2003) Increased phosphorylation of myosin light chain associated with slow-to-fast transition in rat soleus. *Am. J. Physiol. Cell Physiol.* **285,** C575–C583
21. Dubroca, C., Loyer, X., Retailleau, K., Loirand, G., Pacaud, P., Feron, O., Balligand, J. L., Levy, B. I., Heymes, C., and Henrion, D. (2007) RhoA activation and interaction with Caveolin-1 are critical for pressure-induced myogenic tone in rat mesenteric resistance arteries. *Cardiovasc. Res.* **73,** 190–197
22. Schreiber, D. H., and Anderson, T. R. (2006) Statin-induced rhabdomyolysis. *J. Emerg. Med.* **31,** 177–180
23. Kou, R., Sartoretto, J., and Michel, T. (2009) Regulation of Rac1 by simvastatin in endothelial cells: differential roles of AMP-activated protein kinase and calmodulin-dependent kinase kinase-beta. *J. Biol. Chem.* **284,** 14734–14743
24. Wang, W., and Wong, C. W. (2010) Statins enhance peroxisome proliferator-activated receptor gamma coactivator-1alpha activity to regulate energy metabolism. *J. Mol. Med.* **88,** 309–317
25. Arany, Z., Lebrasseur, N., Morris, C., Smith, E., Yang, W., Ma, Y., Chin, S., and Spiegelman, B. M. (2007) The transcriptional coactivator PGC-1beta drives the formation of oxidative type IIX fibers in skeletal muscle. *Cell Metab.* **5,** 35–46
26. Izumo, N., Fujita, T., Nakamuta, H., and Koida, M. (2001) Lipophilic statins can be osteogenic by promoting osteoblastic calcification in a Cbfa1- and BMP-2-independent manner. *Methods Find. Exp. Clin. Pharmacol.* **23,** 389–394
27. Rome, L. C., Sosnicki, A. A., and Goble, D. O. (1990) Maximum velocity of shortening of three fibre types from horse soleus muscle: implications for scaling with body size. *J. Physiol.* **431,** 173–185
28. Puthoff, M. L., and Nielsen, D. H. (2007) Relationships among impairments in lower-extremity strength and power, functional limitations, and disability in older adults. *Phys. Ther.* **87,** 1334–1347
29. Von Tresckow, B., von Strandmann, E. P., Sasse, S., Tawadros, S., Engert, A., and Hansen, H. P. (2007) Simvastatin-dependent apoptosis in Hodgkin's lymphoma cells and growth impairment of human Hodgkin's tumors in vivo. *Haematologica* **92,** 682–685
30. Cohen, G. M. (1997) Caspases: the executioners of apoptosis. *Biochem. J.* **326**(Pt. 1), 1–16
31. Schiaffino, S., and Reggiani, C. (1996) Molecular diversity of myofibrillar proteins: gene regulation and functional significance. *Physiol. Rev.* **76,** 371–423
32. Bottinelli, R., and Reggiani, C. (2000) Human skeletal muscle fibres: molecular and functional diversity. *Prog. Biophys. Mol. Biol.* **73,** 195–262
33. Pellegrino, M. A., Canepari, M., Rossi, R., D'Antona, G., Reggiani, C., and Bottinelli, R. (2003) Orthologous myosin isoforms and scaling of shortening velocity with body size in mouse, rat, rabbit and human muscles. *J. Physiol.* **546,** 677–689
34. Pette, D., and Staron, R. S. (1990) Cellular and molecular diversities of mammalian skeletal muscle fibers. *Rev. Physiol. Biochem. Pharmacol.* **116,** 1–76
35. Bottinelli, R., Betto, R., Schiaffino, S., and Reggiani, C. (1994) Unloaded shortening velocity and myosin heavy chain and alkali light chain isoform composition in rat skeletal muscle fibres. *J. Physiol.* **478**(Pt. 2), 341–349
36. Scott, D., Blizzard, L., Fell, J., and Jones, G. (2009) Statin therapy, muscle function and falls risk in community-dwelling older adults. *QJM* **102,** 625–633
37. Istvan, E. S., and Deisenhofer, J. (2000) The structure of the catalytic portion of human HMG-CoA reductase. *Biochim. Biophys. Acta* **1529,** 9–18
38. Sirvent, P., Bordenave, S., Vermaelen, M., Roels, B., Vassort, G., Mercier, J., Raynaud, E., and Lacampagne, A. (2005) Simvastatin induces impairment in skeletal muscle while heart is protected. *Biochem. Biophys. Res. Commun.* **338,** 1426–1434
39. Payne, A. M., Dodd, S. L., and Leeuwenburgh, C. (2003) Life-long calorie restriction in Fischer 344 rats attenuates age-related loss in skeletal muscle-specific force and reduces extracellular space. *J. Appl. Physiol.* **95,** 2554–2562

Received for publication March 14, 2011.
Accepted for publication July 21, 2011.